Enzyme Kinetics of Cytochrome P450-Mediated Reactions

Magang Shou , Yuh Lin, Ping Lu, Cuyue Tang, Qin Mei, Dan Cui, Wei Tang[#], Jason S. Ngui[#], C. Charles Lin, Rominder Singh, Bradley K. Wong, James A. Yergey, Jiunn H. Lin, Paul G. Pearson, Thomas A. Baillie, A. David Rodrigues and Thomas H. Rushmore

Department of Drug Metabolism, Merck Research Laboratories, West Point, PA 19486 and [#]*Department of Drug Metabolism, Merck Research Laboratories, Rahway, NJ 07065, USA*

Abstract: The most common drug-drug interactions may be understood in terms of alterations of metabolism, associated primarily with changes in the activity of cytochrome P450 (CYP) enzymes. Kinetic parameters such as K_m, V_{max}, K_i and K_a, which describe metabolism-based drug interactions, are usually determined by appropriate kinetic models and may be used to predict the pharmacokinetic consequences of exposure to one or multiple drugs. According to classic Michaelis-Menten (M-M) kinetics, one binding site models can be employed to simply interpret inhibition (pure competitive, non-competitive and uncompetitive) or activation of the enzyme. However, some cytochromes P450, in particular CYP3A4, exhibit unusual kinetic characteristics. In this instance, the changes in apparent kinetic constants in the presence of inhibitor or activator or second substrate do not obey the rules of M-M kinetics, and the resulting kinetics are not straightforward and hamper mechanistic interpretation of the interaction in question. These unusual kinetics include substrate activation (autoactivation), substrate inhibition, partial inhibition, activation, differential kinetics and others. To address this problem, several kinetic models can be proposed, based upon the assumption that multiple substrate binding sites exist at the active site of a particular P450, and the resulting kinetic constants are, therefore, solved to adequately describe the observed interaction between multiple drugs. The following is an overview of some cytochrome P450-mediated classic and atypical enzyme kinetics, and the associated kinetic models. Applications of these kinetic models can provide some new insights into the mechanism of P450-mediated drug-drug interactions.

INTRODUCTION

Enzyme reactions involving one or multiple substrates consist of a sequence of reversible conversions between various enzyme species. Enzyme-catalyzed reactions are complex in that they proceed from an initial set of one, or multiple, reactants to a final set of products via a mechanism comprising more than one elementary reaction with various transition states of the enzyme. The steady-state velocity equation for a given scheme of an enzyme reaction of any complexity can be derived by the method of King & Altman [1]. In the equation, reaction rate is expressed as a function of ligand concentration (substrates, inhibitors, activators, products, and others) with coefficients composed of the rate and dissociation constants of the reaction steps in the scheme. Therefore, the constants describe "site" properties of the enzyme (k_p, V_{max}, K_m, K_i and K_a). The equation gives information on how all the ligands and enzyme in the scheme interact with each other to affect the velocity of the reaction, while the constants, if they are known, describe the kinetic properties of the enzyme.

With the advent of multiple drug treatment, pharmacokinetic drug-drug interactions are more likely and can have significant clinical consequences (drug toxicity or inefficacy)[2]. A key cause of drug-drug interactions is the effect of

*Address corresponding to this author at the WP75A-203, Dept. of Drug Metabolism, Merck Research Laboratories, West Point, PA 19486, USA; Tel: (215)-652-1899; Fax: (215)-652-2410; E-mail: magang_shou@merck.com

1389-2002/01 $28.00+.00

one agent on the activities of key enzymes involved in the metabolism of a second drug, e.g. cytochromes P450 (CYPs or P450s). Two major mechanisms, inhibition and induction of metabolic clearance, usually underlie such interactions. Cytochromes P450 play a major role in the metabolism of a variety of exogenous compounds [3-7]. Cytochromes P450 possess an identical prosthetic group but differ in their apoprotein structures which determine substrate specificity and kinetic properties. The isoform CYP3A4 is of major importance due to its high abundance in human liver, broad substrate specificity, and frequent involvement in clinically relevant drug-drug interactions [4, 8, 9].

Generally, most P450-mediated reactions follow simple Michaelis-Menten kinetics and their kinetic constants (K_m and V_{max}) are easily derived. If the addition of a P450 effector (inhibitor or activator) results in inhibition or activation of the enzyme reaction, a value for K_i or K_a can be determined with suitable kinetic models. It is accepted that these kinetic parameters can be used to predict and understand *in vivo* pharmacokinetic and pharmacodynamic consequences caused by exposure to one or multiple drugs. Although the kinetic expressions for many types of drug interaction, such as competitive, non-competitive, uncompetitive inhibition and direct activation, have been described in detail elsewhere [10], some kinetic observations *in vitro* are not straight-forward, and hamper mechanistic interpretation of the interaction in question. Some P450s, in particular CYP3A4, exhibit the unusual properties, such as substrate activation [11-17], substrate inhibition [18-20], partial inhibition [12, 21, 22], activation [11, 23-30], and differential kinetics [15, 31]. Due to the complexity of such interactions, kinetic models are required that adequately fit the experimental data and yield accurate estimates of kinetic parameters. Recently, multiple binding site models have been proposed and utilized to describe atypical enzyme kinetics [12, 16-18, 29, 31]. In this instance, kinetic constants can be obtained by non-linear regressions (*Axum* 5.0, *Mathematica* 4, *SigmaPlot* 5.0, *SigmaPlot* 2000, *Grafit* 3.09, *KaleidaGraph* 3.09 and others).

MICHAELIS-MENTEN KINETICS (ONE-SITE MODEL)

The Michaelis-Menten model assumes that the active site of an enzyme contains one binding site, at which the catalytic process occurs, and the velocity of the reaction can be characterized as a hyperbolic saturating profile [10]. The approach (Scheme I and Eqn. 1) is applied commonly to

$$E + S \underset{k_{-1}}{\overset{k_1}{\rightleftharpoons}} ES \xrightarrow{k_p} E + P$$

(Scheme I). A typical Michaelis-Menten kinetic model. E = enzyme, S = substrate, $K_m = (k_{-1}+k_p)/k_1$ and $V_{max} = k_p [E]_{total}$. The velocity equation is given in the text as Eqn. 1.

most enzymes in a biological environment. The enzyme reaction must meet both steady state and rapid equilibrium assumptions, e.g. $+d[ES]/dt = k_1[E][S] = -d[ES]/dt = (k_{-1}+k_p)[ES]$. Therefore, K_m $\{(k_p+k_{-1})/k_1\}$ and V_{max} $(k_p[E]_{total})$ can be estimated, respectively, by non-linear regression of the typical hyperbolic velocity curve. The kinetics of (S)-mephenytoin 4'-hydroxylation are given as an example in (Fig **1**). To acquire accurate constants, substrate concentrations must be chosen around

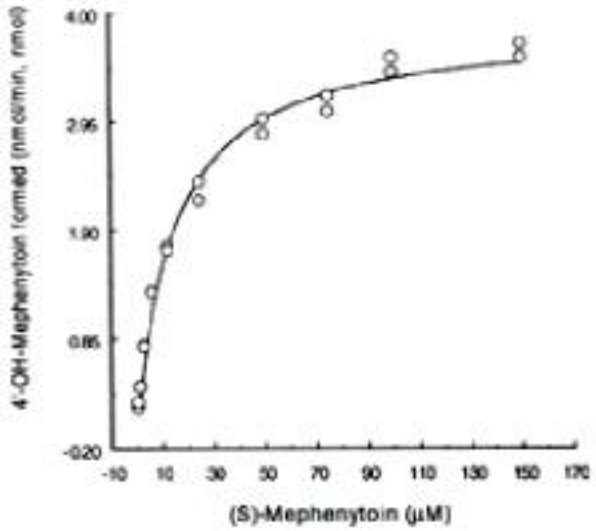

Fig. (1). Hyperbolic saturation curve of CYP2C19-catalyzed (*S*)-Mephenytoin 4'-hydroxylation. K_m and V_{max} values were calculated with Eqn. 1 (K_m = 23.7 ± 2.15 μM and V_{max} = 0.36 ± 0.01 nmol/min, nmol). Data were fitted by non-linear regression (Eqn. 1).

the K_m value and the observed velocity curve should be hyperbolic.

$$\upsilon = \frac{V_{max}[S]}{K_m + [S]} \qquad (1)$$

When an effector (inhibitor or activator) is added to the enzyme reaction, the reaction mixture may comprise more than one enzyme complex, namely ES, EI and/or ESI (Scheme II). Since the ES concentration ([ES]) decreases with increases in [I] or [A]. the rate of product formation (k_p[ES]) can either decline ($0 \leq \beta < 1$) or increase ($\beta > 1$) depending on the nature of the effector. Scheme II depicts a general kinetic model used to describe the interaction between substrate, effector (inhibitor) and enzyme. For competitive inhibition, S and I compete with each other for the active site and only ES and EI complexes exist. Their concentrations, [ES] and [EI], vary with the concentration of the competitors, [S] and [I]. Competitive inhibition (Eqn. 2) is characterized by changes in apparent K_m (increase) and V_{max} values (unchanged) with respect to [I]. Celecoxib is a competitive inhibitor of CYP2C19 in (*S*)-mephenytoin 4'-hydroxylation (Fig. **2** and **3**). Fig. 2 shows the fitting of predicted results (surface

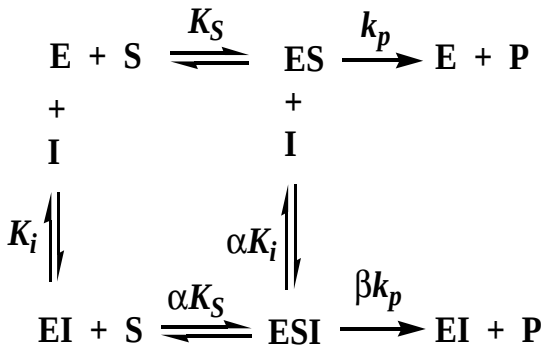

(Scheme II). General kinetics for competitive ([ESI] = 0), non-competitive ($\alpha = 1$ and $\beta = 0$), uncompetitive ($\alpha = 1$, $\beta = 0$ and [EI] = 0), and mixed type inhibition ($\alpha \neq 1$ and $0 < \beta < 1$). K_S = dissociation constant for substrate (S); K_i = dissociation constant for inhibitor (I); k_p = rate constant for the formation of product; α and β are factors that change K_S or K_i and k_p when the second molecule (either I or S) is bound. Rate equations for above inhibition kinetics are given in the text as Eqn. 2 (competitive), 3 (non-competitive), 4 (uncompetitive) and 5 (mixed-type).

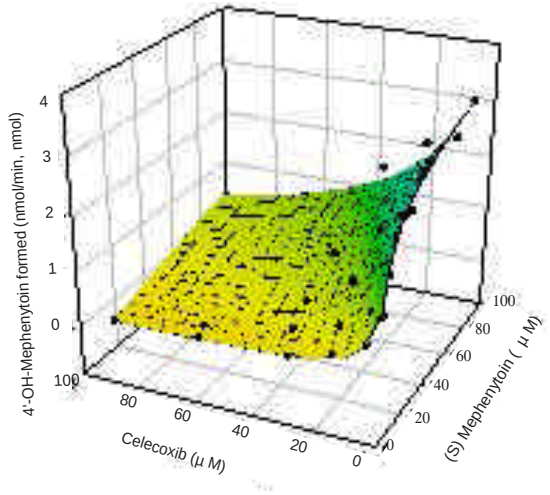

A

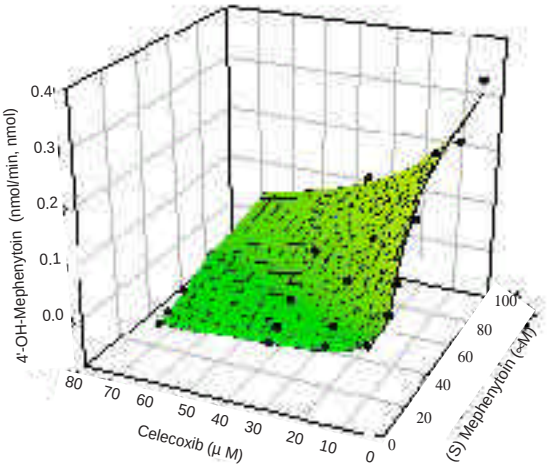

B

Fig. (2). (**A**) Celecoxib inhibition of recombinant CYP2C19-catalyzed (*S*)-mephenytoin 4'-hydroxylation: V_{max} = 3.7 ± 0.2 nmol/min, nmol, K_S = 9.8 ±1.9 μM, K_i = 3.3 ± 0.6 μM, *RSS* (Residual Sum of Squares) = 0.935, and R^2 = 0.965, respectively. (**B**) Celecoxib inhibition of CYP2C19-catalyzed (*S*)-mephenytoin 4'-hydroxylation in human liver microsomes: V_{max} = 0.40 ± 0.02nmol/min, nmol, K_S = 13.8 ± 1.9 μM, K_i = 3.2 ± 0.4 μM, *RSS* = 0.002, and R^2 = 0.981, respectively. All kinetic values were determined by multiple non-linear regression using Eqn. 2.

plots) with experimental data (scatter points). K_m, V_{max} and K_i, therefore, were obtained using Eqn. 2 as shown in the legend of Fig. 2.

$$\upsilon = \frac{V_{max}[S]}{K_S(1 + \frac{[I]}{K_i}) + [S]} \qquad (2)$$

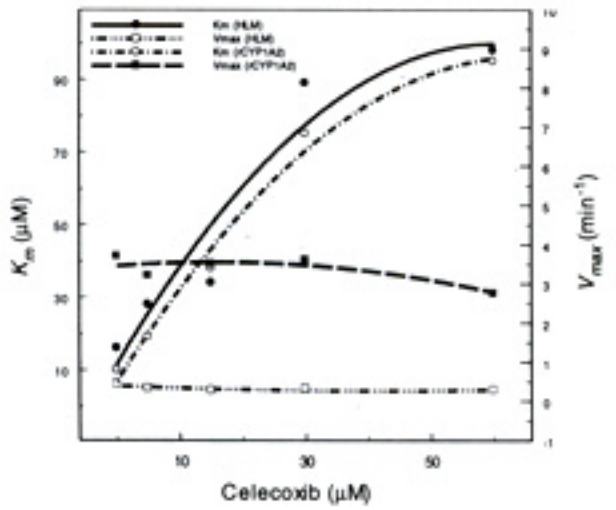

Fig. (3). Competitive inhibition of celecoxib in CYP2C19-catalyzed (*S*)-mephenytoin 4'-hydroxylation by recombinant CYP2C19 and human liver microsomes, respectively, showing increased apparent K_S and unchanged V_{max} with respect to inhibitor concentrations.

If the inhibition is purely non-competitive, both EI and ES complexes can combine subsequently with a second molecule to form ESI, that is believed to be non-productive ($\beta = 0$, $\alpha = 1$). Typically, the apparent K_m is unchanged and V_{max} decreases as [I] increases. Monoclonal antibody (MAb)-mediated P450 inhibition was found to be mainly non-competitive, based on the observed change in apparent constants (Fig. **4**). The K_i for anti-CYP3A4 MAb is 3 nM, determined by Eqn. 3, a value which is much smaller than that observed with chemical inhibitors.

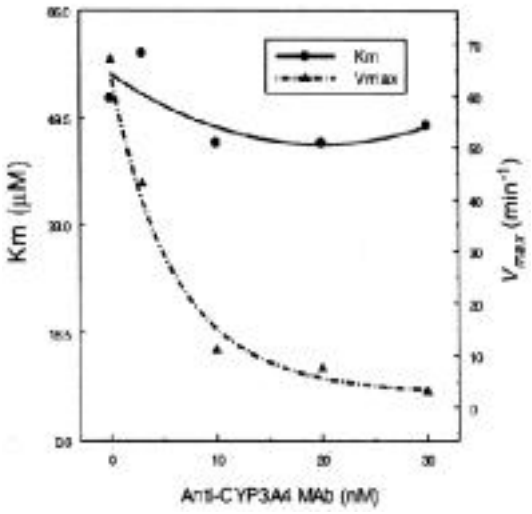

Fig. (4). Non-competitive inhibition by anti-CYP3A4 monoclonal antibody of CYP3A4-catalyzed testosterone 6β-hydroxylation (unchanged apparent K_S and decreased V_{max} when inhibitor concentration increases). K_i = 3.0 ± 0.12 nM (Eqn. 3).

$$\upsilon = \frac{V_{max}[S]}{K_S(1+\frac{[I]}{K_i}) + [S](1+\frac{[I]}{K_i}\}} \qquad (3)$$

Un-competitive inhibition is rare in practice, although inhibition of CYP1A2-mediated phenacetin *O*-deethylation in the presence α-naphthoflavone (α-NF) is an example (Fig. **5**). By definition, as the concentration of inhibitor increases, both apparent K_m and V_{max} decrease: ESI complex formation occurs only after the formation of ES ($\alpha = 1$ and $\beta = 0$). Thus, the reaction contains only ES and ESI and the velocity equation is written as Eqn. 4. Kinetic constants, determined by Eqn. 4, are listed in the legend to Fig. 5.

$$\upsilon = \frac{V_{max}[S]}{K_S + [S](1+\frac{[I]}{K_i})} \qquad (4)$$

In general, three types of inhibition kinetics are recognized according to the changes in observed apparent constants. In fact, it is commonly observed in P450-mediated reactions that (1) inhibition of a reaction is partial at the saturating level of inhibitor ($0 < \beta < 1$, Scheme II), or (2) dissociation constants (K_i and K_S) are altered by factor α ($\alpha \neq 1$), when a second molecule binds to the enzyme, resulting in two different values for K_i and K_S (K_i, αK_i, K_S and αK_S), respectively, or (3) both situations can exist ($\alpha \neq 1$ and $0 < \beta < 1$), resulting in mixed type inhibition. This inhibition results from direct or indirect interaction between substrate and inhibitor within an enzyme, depending on the physical and chemical properties of the ligands, ie, shape, size and allosteric effect. Eqn. 5 is an expression for mixed type inhibition. The changes in apparent K_m and V_{max} associated with this inhibition are different from those observed with any of the above types of inhibition, with respect to inhibitor concentrations. Factors α and β, which represent changes in K_i or K_S and V_{max} in the presence of inhibitor ($\alpha \neq 0$ and $0 <$

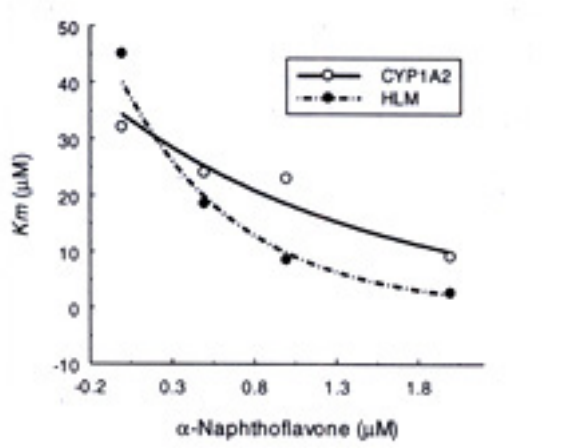

A

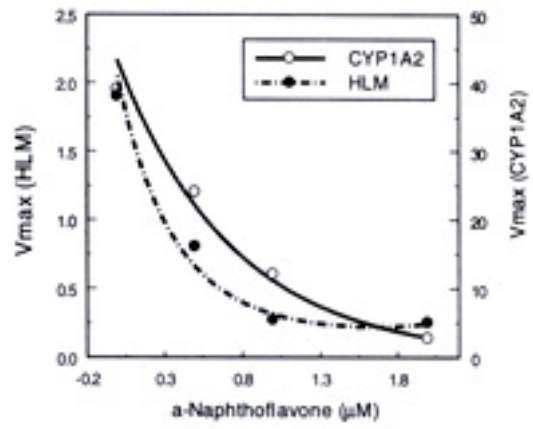

B

Fig. (5). Un-competitive inhibition by α-naphthoflavone of CYP1A2-catalyzed phenacetin *O*-deethylation in recombinant CYP1A2 and human liver microsomes, respectively (**A**: decreased apparent K_S and **B**: V_{max}). K_i = 0.57 ± 0.04 μM for HLM and 0.31 ± 0.06 for rCYP1A2, respectively (Eqn. 4).

β < 1), are important in considering binding affinity and inhibition potency of the inhibitor for the enzyme. This will be described in the following section on the two-site model. Since the equation contains five unknowns, accurate determination of the constants requires adequate experimental points for a regression and, thus, 6-8 points each for [S] and [I] (total = 36 –64 points) are desired.

$$\upsilon = \frac{V_{max}(\frac{[S]}{K_S} + \frac{\beta[S][I]}{\alpha K_S K_i})}{1 + \frac{[S]}{K_S} + \frac{[I]}{K_i} + \frac{[S][I]}{\alpha K_S K_i}} \quad (5)$$

P450 activation can be expressed by the same kinetic model of Scheme II when effector acts as an activator (A). In this case, ESI in the scheme can be replaced by ESA which is more productive than ES, and factor β, therefore, must be greater than one (β > 1). It is noted that in the Michaelis-Menten model, I or A is not assumed to bind simultaneously with substrate to the catalytic site of the enzyme.

In the pharmaceutical industry, new chemical entities (NCEs) are screened *in vitro* for their ability to inhibit P450 isoforms and attempts are made to predict the potential of clinical drug-drug interactions. The IC_{50} value, the concentration of the inhibitor that gives 50% of maximal inhibition of an individual P450 activity, usually is employed as an estimate of the P450 inhibitory potency, since the measurement of IC_{50} is simple and rapid. If the mechanism of the inhibition is known, the IC_{50} value also can be used to evaluate K_i. The mathematical expressions (% of control) for competitive, non-competitive and uncompetitive inhibition kinetics are given in Eqn. 6, 7 and 8, respectively.

$$Control\% = \frac{\upsilon_i}{\upsilon_0} = \frac{K_m + [S]}{K_m(1 + \frac{[I]}{K_i}) + [S]} \quad (6)$$

$$Control\% = \frac{\upsilon_i}{\upsilon_0} = \frac{K_m + [S]}{(K_m + [S])(1 + \frac{[I]}{K_i})} \quad (7)$$

$$Control\% = \frac{\upsilon_i}{\upsilon_0} = \frac{K_m + [S]}{K_m + [S](1 + \frac{[I]}{K_i})} \quad (8)$$

As seen from the equations, percent inhibition is a function of both [S] and [I]. When [S] approaches K_m ([S] = K_m), the above eqations can

be simplified greatly, and therefore, IC_{50} is essentially equal to $2K_i$ for both competitive and uncompetive inhibition, and to K_i for non-competitive inhibition. However, the IC_{50} value cannot be used as an estimate of K_i in the mixed type inhibition, due to the interference of factors α and β (Scheme II).

ATYPICAL ENZYME KINETICS (TWO-SITE MODEL)

Cytochromes P450, particularly CYP3A4, are characterized by a broad substrate specificity. Substrates range from generally small to large in size (up to 1,200 Dalton), and typically are highly lipophilic. K_m values for substrates vary markedly between 1 and 1,500 μM. A number of workers have derived models for the active sites of human P450s, based on either superposition of known substrates or sequence homologies with known crystal structures of P450s as templates [32, 33]. Others have explored P450 active sites using molecular probes [34]. In some cases, considerable changes in the active site regions of different isoforms have been observed, which reflect the different substrate specificities, especially due to size and shape considerations. The CYP3A4 model shows a large active site with a well-defined access channel for substrates, in keeping with the known preference of this enzyme for large, structurally diverse substrates. Even the cyclosporin molecule, which is of considerable size relative to substrates for other P450s, is accomodated by the CYP3A4 site [29]. This observation suggests that the active site of CYP3A4 may accommodate two or more intermediate-sized substrate molecules for metabolism. This hypothesis is supported by numerous kinetic observations [11, 12, 14-17, 20, 22, 23, 27, 28, 31, 35-38]. Atypical kinetics can be explained by multiple binding site models. For instance, the two-site model hypothesizes that two substrate molecules of the same or different chemical entity can bind simultaneously to two distinct portions of the active site, and either of the two substrates can be metabolized through interaction with the reactive oxygen, which is bound to the heme iron. When two molecules co-exist within the active site, some interactions may occur between them, due to steric, electronic or allosteric effects, leading to an alteration of kinetic properties (apparent K_m, K_i and V_{max}). Appropriate kinetic models for various drug interactions can be postulated according to the observed change in apparent constants. Data fitting to the models and the resulting constants can be achieved by non-linear regression and statistical analysis.

Substrate Activation

Evidence has accumulated in recent years to support the concept of allosteric interactions involving the substrate (activator) itself. It is believed that positive cooperativity is due to alterations of the substrate or the activator binding site of an enzyme as a result of activator-induced conformational changes, resulting in enzyme activation (sigmoidal saturation curve). To our knowledge, no attempts have been made to delineate the nature of the alterations at the binding site. Most of the examples reported to date have been attributed to CYP3A4, e.g. the metabolism of aflatoxin B1 [15], steroids [37, 39], carbamazepine [12, 40], amitriptyline [41], triazolam [17] and diazepam [16, 42]. Therefore, a velocity equation has been derived from the two-site model proposed by Korzekwa (Scheme III) to describe sigmoidal kinetics (Eqn. 9) and to obtain kinetic parameters (e.g. K_{m1}, K_{m2}, V_{max1} and V_{max2}) by non-linear regression (12).

$$\upsilon = \frac{\frac{V_{\max 1}[S]}{K_{m1}} + \frac{V_{\max 2}[S]^2}{K_{m1}K_{m2}}}{1 + \frac{[S]}{K_{m1}} + \frac{[S]^2}{K_{m1}K_{m2}}} \qquad (9)$$

K_{m1} and K_{m2} (Eqn. 9) represent dissociation constants for E+S⇌ES and ES+S⇌ESS equilibria and, accordingly, V_{max1} and V_{max2} represent the maximal velocities for ES and ESS, respectively.

However, conformational changes of the two sites, with subsequent binding of a sigmoidal ligand, can also be considered. In an attempt to define the binding of S to E in a different orientation (SE ≠ ES), an additional two-site model has been proposed (Scheme IV) for

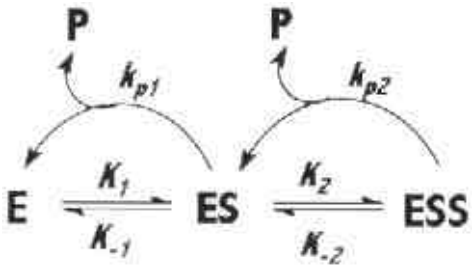

(Scheme III). Proposed kinetic scheme for a P450 enzyme with two binding domains within the active site (substrate activation). The velocity equation is given in the text (Eqn. 9) and kinetic parameters are calculated as shown in Table 1.

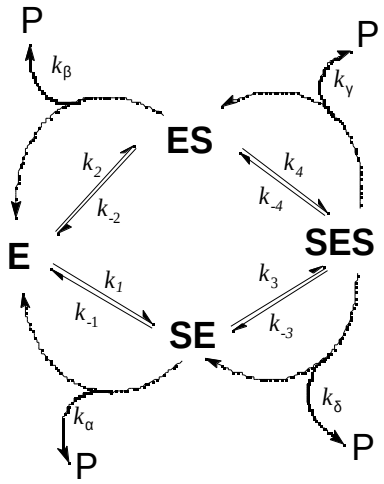

(Scheme IV). Proposed allosteric kinetic scheme for CYP3A4 with two binding domains in the active site (substrate activation). Calculated parameters are shown in Table 2 using Eqn. 10**.**

sigmoidal kinetics [16]. The model postulates that if both sites are cooperative, then the resulting kinetic characteristics of the SES species might differ from those observed for both single SE and ES species. Thus, four pairs of dissociation and rate constants can be generated to explain all possible combinations of singly- and doubly-bound substrate-enzyme species, (Scheme IV, Eqn. 10), e.g. ES, SE and SES.

$$\frac{\upsilon}{[E]_{total}} = \frac{\frac{k_\alpha}{K_{s1}} + \frac{k_\beta}{K_{s2}} + \frac{[S]}{K_{s1}K_{s3}}\,(k_\delta + k_\gamma)}{\frac{1}{[S]} + \frac{1}{K_{s1}} + \frac{1}{K_{s2}} + \frac{[S]}{K_{s2}K_{s4}}} \quad (10)$$

Because the equation contains eight constants, an adequate number of data points is needed to solve the unknowns and to ensure accurate estimates of kinetic parameters. The two Schemes (Schemes III and VI) of the two-site model have been compared to understand the mechanism of CYP3A4-mediated sigmoidal kinetics using diazepam and its metabolites, temazepam and nordiazepam, as substrates (Fig. **6**). Interestingly, the two sets of data were found to be in general agreement (Tables **1** and **2**, Fig. **7**), showing that the singly-bound species (ES and SE) had both poorer binding affinity and catalytic capacity than the SES or ESS. The increase in binding affinity and in catalytic rate of the CYP3A4 for the second substrate molecule probably may be attributed to binding of first substrate to the active site, which induces enzyme cooperativity. Thus, the SES complex of two tightly bound substrates allows the substrate to be readily metabolized. Scheme IV also describes the kinetic discrepancy between the two single-bound sites on the enzyme. For example, in the conversion of DZ to TMZ by CYP3A4 (Table **2**), K_{S2} and k_β for ES were 2.5-fold and 28-fold greater than the K_{S1} and k_α for SE, respectively. This implies that ES disociated more readily to E and S as well as to form product (P). Similarly, the K_{S3} and k_δ values were three-fold greater and two-fold less than those of K_{S4} and k_γ, respectively, indicating that binding of S to ES was tighter than that of S to SE, and that the rate of SES → ES + P was faster than that of SES → SE + P. In general, the binding of substrate to a stereospecific site on an enzyme may result in a modification of another enzyme site which is topographically separate from the first. Thus, an investigation of the nature of the modification of the binding site during an allosteric transition is of fundamental importance towards gaining an understanding of the molecular mechanism of allosteric interaction.

Substrate Inhibition

A substrate that causes a decrease in the rate of product formation as its concentration increases will lead to a reaction that displays substrate inhibition kinetics. Although the mechanism of

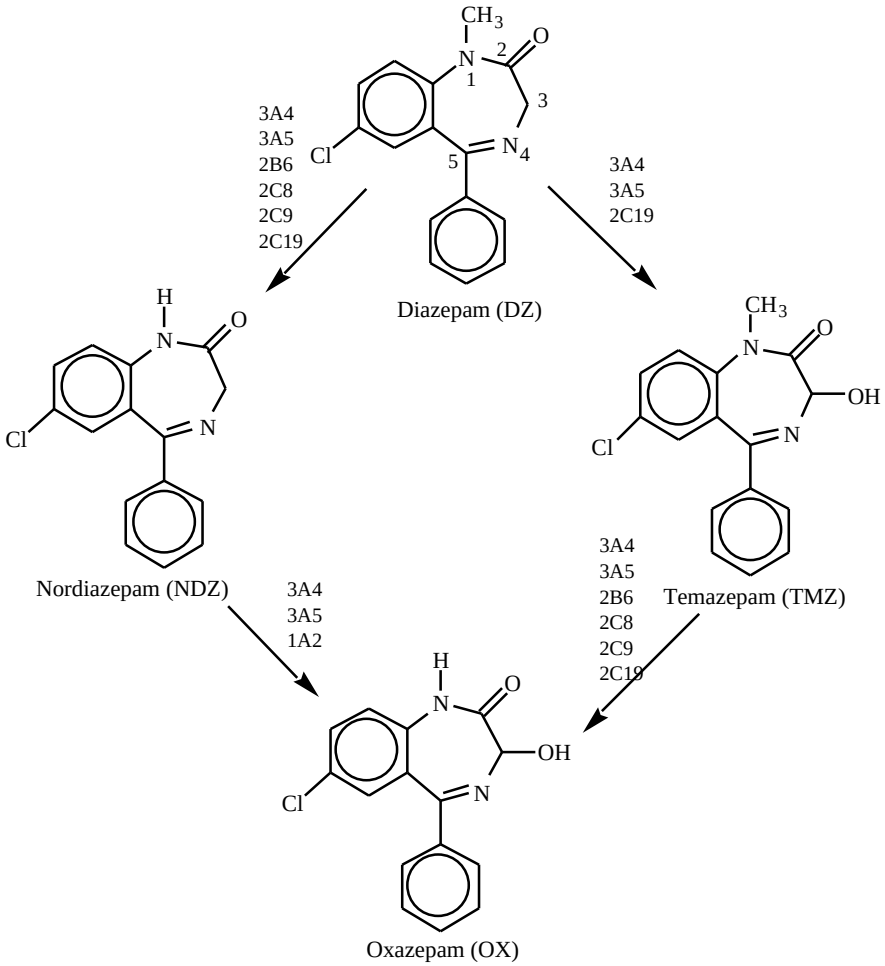

Fig. (6). Involvement of different cytochrome P450 isoformes in the metabolism of diazepam [42].

Table 1. Kinetic Estimates of Sigmoidal Saturation Curves Determined by Eqn. 9

Substrate	Product	Enzyme	K_{m1}[a]	V_{max1}[b]	K_{m2}	V_{max2}	RSS[c]	R^2
DZ	TMZ	3A4[d]	356 (32)	2.1 (0.8)	11.4 (2.3)	24.2 (12.1)	1.2201	0.998
	NDZ	3A4	284 (63)	1.4 (0.3)	18.7 (3.2)	4.8 (1.1)	0.3022	0.999
TMZ	OX	3A4	581 (139)	1.31 (0.12)	33.3 (1.4)	3.5 (1.5)	0.1145	0.998
NDZ	OX	3A4	164 (65)	3.7 (1.1)	24.4 (6.8)	4.8 (0.5)	0.3321	0.996

[a]K_m (apparent, μM) and standard error in parenthesis; [b]V_{max} (nmol/min,nmol); [c]Residual sum of squares; [d]cDNA-expressed CYP3A4.

Table 2. Kinetic Estimates of Sigmoidal Saturation Curves Determined by Eqn. 10

Sub.	Prod.	Enz.	K_{S1}[a]	k_α[b]	K_{S2}	k_β	K_{S3}	k_δ	K_{S4}	k_γ	RSS[d]	R^2
DZ	TMZ	3A4[e]	170 (135)	1.8 (1.4)	421 (233)	49.6 (10)	39.6 (24.7)	392 (94)	13.1 (5.3)	808 (182)	0.7611	0.999
	NDZ	3A4	125 (63)	5.6 (0.6)	329 (21)	4.5 (2.4)	28.1 (5.1)	111 (44)	8.9 (3.2)	49.2 (22.4)	1.020	0.997
TMZ	OX	3A4	482 (43)	10 (14)	830 (31)	29.6 (1.0)	23.3 (3.5)	76 (3.8)	16.5 (2.1)	76 (24)	0.3509	0.992
NDZ	OX	3A4	109 (29)	10.2 (4.1)	168 (31.5)	39.2 (9.3)	20.2 (31.5)	30.2 (22.2)	25.1 (2.3)	102 (33)	0.1327	0.992

[a]K_S (apparent, μM) and standard error in parenthesis and all kinetic coefficients are defined by the Scheme IV and Eqn. 10 ; [b]k_α (nmol/min,nmol); [d]Residual sum of squares; [e]Baculovirus-expressed CYP3A4.

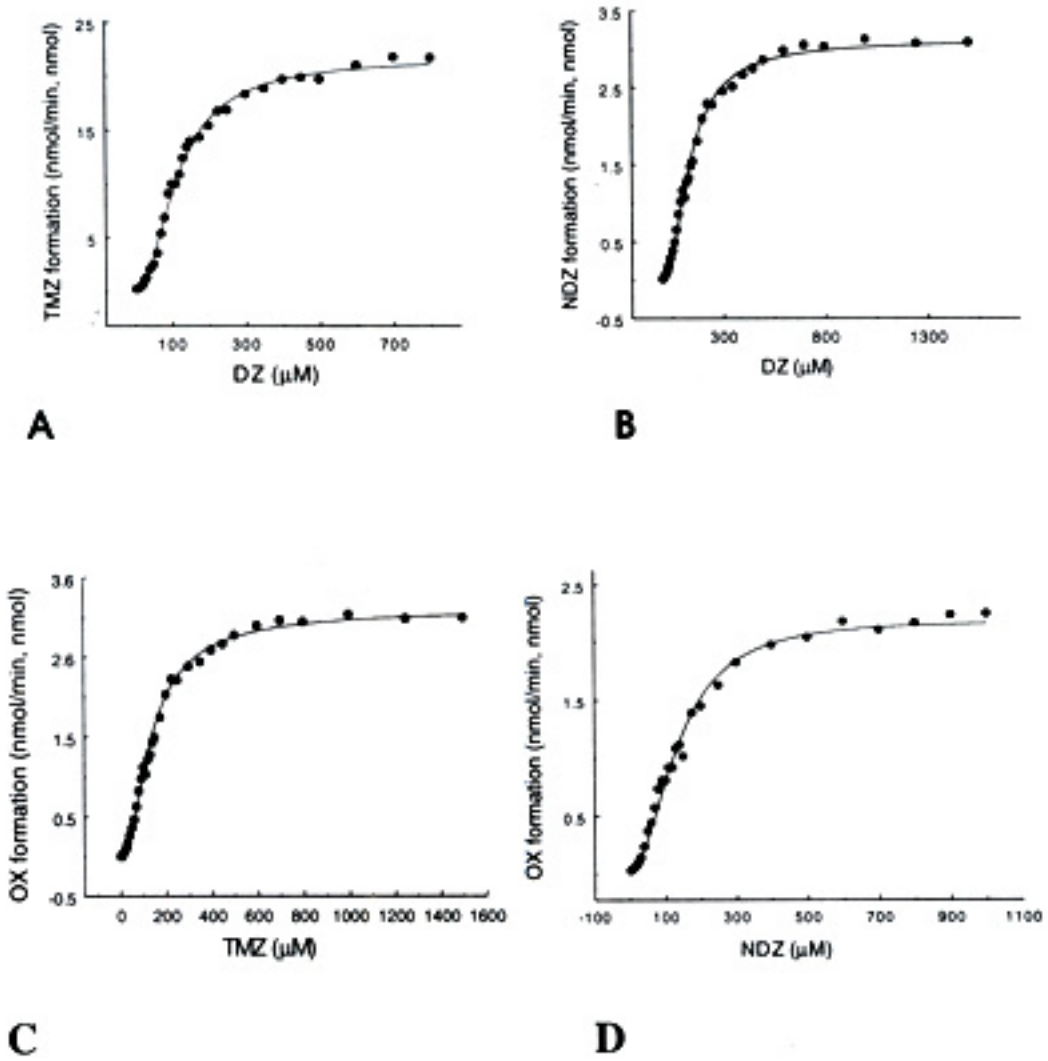

Fig. (7). Sigmoidal saturation curve of velocity vs. [S] for the recombinant CYP3A4-catalyzed metabolism of DZ, TMZ and NDZ, respectively. **A**: DZ conversion to TMZ; **B**: DZ conversion to NDZ; **C**: TMZ conversion to OX and **D**: NDZ conversion to OX. Predicted parameters are given in Table 2 (Eqn. 10).

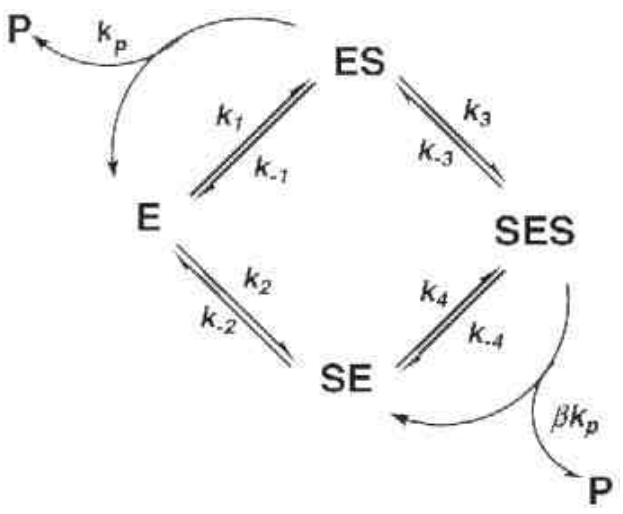

(Scheme V). Kinetic model for substrate inhibition. When S binds to the catalytic site of the enzyme (ES), the rate and V_{max} of product formation (ES → P) are determined by k_p[ES] and $k_p[E]_{total}$, respectively. When S binds to the inhibitory site (SE) that is non-productive, the rate of SES → P is determined by factor β (0 < β <1). Dissociation constants for all species are defined by $K_S = k_{-1}/k_1$, $K_i = k_{-2}/k_2$, $\alpha K_i = k_{-3}/k_3$ and $\alpha K_S = k_{-4}/k_4$. All parameters are shown in Table 3 using Eqn. 11.

P450-mediated substrate inhibition remains unknown, ignoring the phenomenon and truncating the data can result in substantial errors in the values derived for critical kinetic parameters [18]. To address this issue, a two-site model can be proposed (Scheme V). In this kinetic scheme, the term ES denotes substrate binding to the active site of the enzyme that is productive (k_p). The SE term denotes binding of substrate to the inhibitory site of the enzyme that reduces the rate of enzyme catalysis. The inhibitory site is assumed to be non-productive ($k_p \rightarrow 0$ for SE). The term SES denotes that the two sites are occupied with substrates. Once the inhibitory site is bound by excess substrate, the turnover for SES no longer is the same as that of ES, and is reduced by factor β (usually $0 < \beta < 1$) that determines the potency of the inhibition. The derived equation is shown below (Eqn. 11).

$$\upsilon = \frac{V_{max}\left(\frac{1}{K_S} + \frac{\beta[S]}{\alpha K_i K_S}\right)}{\frac{1}{[S]} + \frac{1}{K_S} + \frac{1}{K_i} + \frac{[S]}{\alpha K_S K_i}} \qquad (11)$$

Table 3. Calculated Kinetic Parameters of the Substrate Inhibition Kinetics (Eqn. 11)

Substrate	P450[a]	Product	Parameters[b]						
			α	K_S	K_i	β	V_{max}	RSS	R^2
Ethoxyresorufin	1A2[c]	Resorufin	8.1±2.3	5.3±1.1	25.5±8.3	0.03±0.01	733±58	26.8	0.988
Celecoxib	2C9	Hydroxycelecoxib	23.3±4.1	5.8±2.3	16.4±3.2	0.08±0.03	10.6±2.4	1.26	0.991
	2C9*2	Hydroxycelecoxib	12.2±2.8	8.2±3.2	10.2±2.8	0.11±0.05	7.2±1.8	0.31	0.989
	2C9*3	Hydroxycelecoxib	5.1±3.1	4.5±1.8	24.6±3.8	0.05±0.01	1.3±0.5	0.02	0.993
Dextrometh-orphan	2D6	Dextrophan	23.8±5.6	4.8±0.6	48.4±6.7	0.12±0.06	4.3±0.9	1.83	0.976
Testosterone	3A4	6β-OH-Testosterone	5.7±1.2	46±21	263±34	0.61±0.21	36±28	10.1	0.992
Progesterone	3A4	6β-OH-Progesterone	13.2±3.6	16.2±4.9	96±25	0.41±0.14	37±11	2.69	0.996
Benzyloxy-resorufin	3A4	Resorufin	6.3±3.2	6.1±2.1	39±12	0.08±0.02	231±59	3.1	0.981

[a]Baculovirus-expressed individual P450s; [b] Parameters are defined by the Scheme V; [c]Baculovirus-expressed P450s.

where $V_{max} = k_p [E]_{total}$, $K_m \approx K_S = k_{-1}/k_1$ ($k_p << k_{-1}$) and $K_i = k_{-2}/k_2$. K_S and K_i are dissociation constants of substrate binding to the catalytic site (ES) and to the inhibitory site (SE), respectively. α and β represent the factors by which the dissociation (K_S and K_i) of substrate at both sites, and the maximal velocity (V_{max}) at the catalytic site, change when a second substrate is bound, i.e. $\alpha K_S = k_{-3}/k_3$, $\alpha K_i = k_{-4}/k_4$, $\beta V_{max} = \beta k_p [E]_{total}$.

As seen in Fig.8, A through F, studies have shown that the data for substrate inhibition can be fitted to the two-site model. The resulting kinetic constants can be used to interpret the nature of the substrate inhibition. Several common features are apparent (Table **3**): (1) K_S values generally are less than K_i, suggesting that the substrate has a binding affinity greater than that of the inhibitor; (2) when both sites are bound, the two constants for the single bound complexes can be altered as determined by factor α (usually $\alpha > 1$). This suggests that the affinity of the substrate for the doubly-bound complex is less than that for the singly-bound complexes; and (3) accordingly, the maximum velocity (V_{max}) of the ES complex can be changed to βV_{max} for SES ($0 < \beta < 1$, Table **3**), which is less able to convert substrate to product than ES. The maximum inhibition is given by β ($0 < \beta < 1$) when [SES] approaches $[E]_{total}$. Our results have shown that β values range between 0.03 and 0.61, leading to a maximum inhibition (39 - 97%). Thus, the magnitude of substrate inhibition at a given concentration is dependent upon the ratio of [ES] to [SES]. Furthermore, the potency of substrate inhibition can be expressed in terms of the interaction of the two-bound substrates with the enzyme.

It is not uncommon to find that, while M-M kinetics are obeyed at lower substrate concentrations, the velocity of the reaction falls off at high concentrations (Fig. **8**). At low concen-

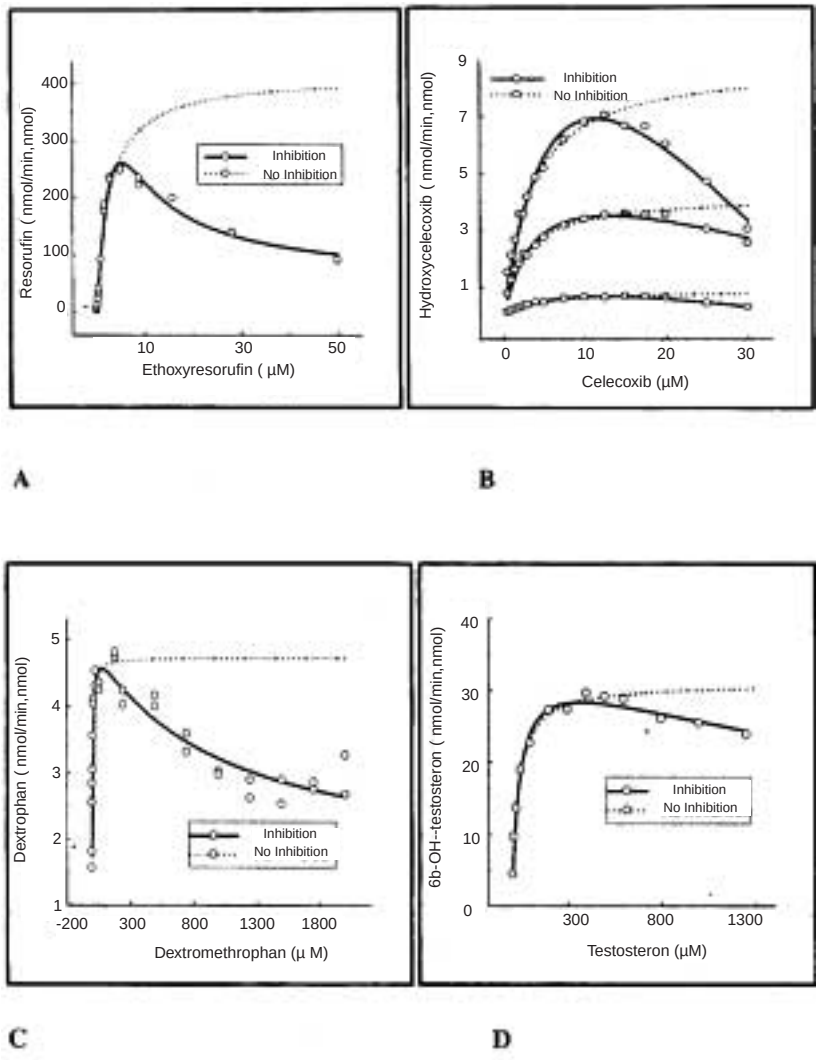

(Fig. 8)…contd.

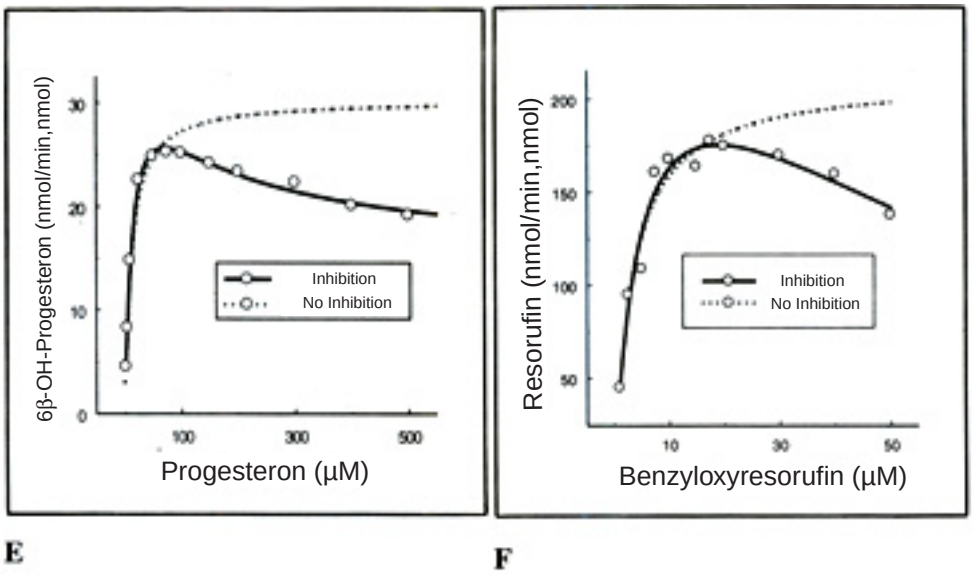

Fig. (8). Substrate inhibition of CYP-catalyzed reactions. Dotted lines represent hyperbolic saturation curves fitted to the Michaelis-Menten equation (Eqn.1) after truncating the inhibited rates at high substrate concentrations, and solid lines represent substrate inhibition curves fitted to Eqn 11. All calculated parameters are shown in Table 3 (Eqn. 11). **A:** CYP1A2-catalyzed *O*-deethylation of ethoxyresorufin; **B**: CYP2C9-catalyzed methyl-hydroxylation of celecoxib. Curves (from top to bottom) represent wild type CYP2C9, CYP2C9*2($_{Arg\_Cys}^{144}$) and CYP2C9*3 ($_{Ile\_Leu}^{359}$), respectively; **C**: CYP2D6-catalyzed *O*-demethylation of dextromethorphan; **D**: CYP3A4-catalyzed 6β-hydroxylation of testosterone; **E**: CYP3A4-catalyzed 6β-hydroxylation of progesterone; and **F**: CYP3A4-catalyzed *O*-dealkylation of benzyloxyresorufin.

trations of the substrate, the effective enzyme-substrate complex would be mainly accounted for due to its low K_m. Thus, at low substrate concentrations, the substrate molecule binds readily to the enzyme to form the ES product-forming complex and the reaction rate is a function of the ES concentration. The data conform to classical Michaelis-Menten kinetics. At high substrate concentrations ($> K_i$), where the substrate molecules tend to crowd on to the enzyme, the chance of formation of ineffective complexes with two substrate molecules increases, resulting in inhibition even though $K_i > K_S$. In fact, substrate inhibition appears only at the concentrations of substrate adequate for binding to the inhibitory site.

Partial Inhibition

Partial inhibition reflects incomplete inhibition, in which the enzyme is saturated with inhibitor. This phenomenon is commonly encountered in P450-catalyzed reactions and corresponds to a mixed-type inhibition. The cause of the partial inhibition is the formation of a substrate-inhibitor-enzyme complex (ESI, Scheme II) that is productive (ESI $\rightarrow$ P). The kinetics can be understood in terms of either the one-site or two-site model, depending on where the inhibitor binds i.e. the non-active site or active site. In the one-site model, the inhibitor binds to the non-active site and then inhibits enzyme activity. Partial inhibition may result from either a conformational change of the enzyme that alters the binding affinity for substrate, or steric hindrance that hampers substrate access to the active site. The two-site model considers that inhibitor and substrate can bind simultaneously to the two distinct sites within a catalytic P450 pocket, and their interaction in the interior of the enzyme can result in partial inhibition. Scheme II and Eqn. 5 describe a general kinetic scheme of both models. Factors α and β ($0 < \beta < 1$) in the model represent the change in K_S (K_i) and V_{max} for substrate when the inhibitor occupies the enzyme. In this case, the K_i (K_i and αK_i) and β values are important estimates of P450 inhibition. If $\alpha \neq 1$, the two K_i values can be obtained through data fitting. As a matter of fact, the potency of P450 inhibition relies on inhibitor and substrate interaction. For

example, (Fig. **9A** and **9B**) show an inhibitor (Inhibitor X, K_i = 10 – 15 μM) that inhibited maximally the CYP3A4-catalyzed 6β-hydroxylation of testosterone by 32% (β = 0.68, Table **4**), but taxol 3'-hydroxylation by 48% (β = 0.52),

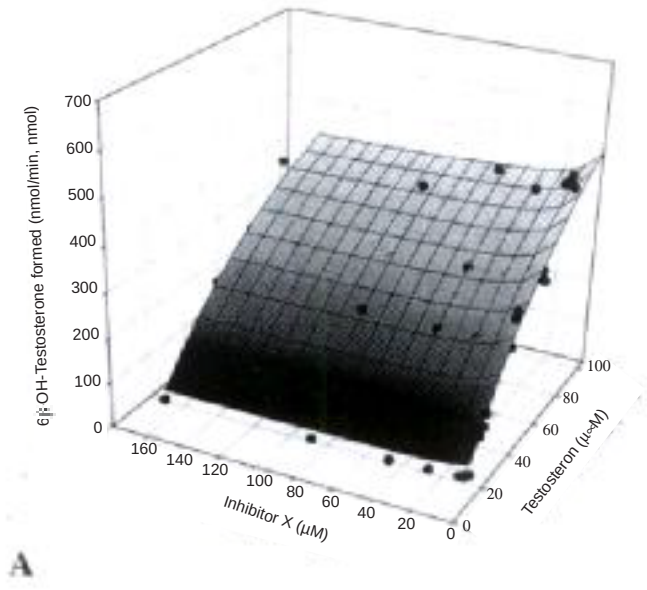

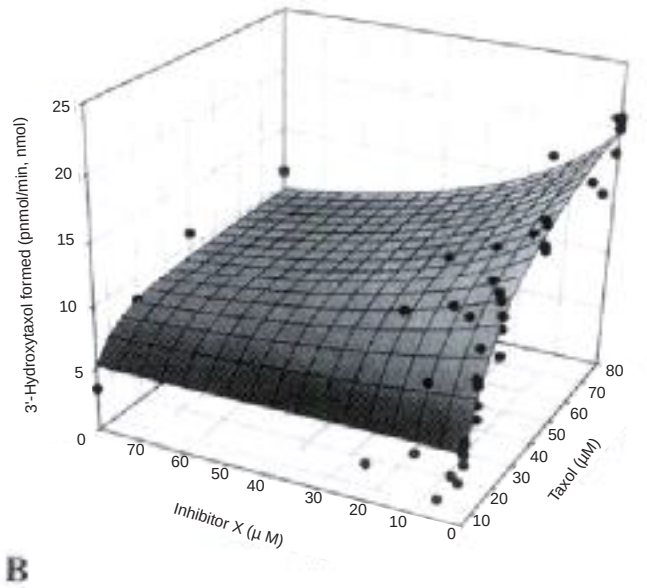

Fig. (9). Partial inhibition kinetics of Inhibitor X for CYP3A4-catalyzed reactions (**A**: testosterone 6β-hydroxylation and **B**: taxol 3'-hydroxylation) in human liver microsomes. The surface plots are the predicted results and scatter plots are experimental observations. Predicted kinetic parameters are shown in Table 4 (Eqn. 5).

Table 4. Predicted Kinetic Parameters for Partial Inhibition Kinetics (Eqn. 5)

Parameters[a]	Testosterone 6β-hydroxylation[b]	Taxol 3'-hydroxylation
V_{max} (pmol/min, mg)	958.3±101.9	23.8±1.2
K_S (μM)	95.06±19.14	15.0±2.2
K_i (μM)	9.7±3.8	15.1±11.7
α	0.97±0.32	1.2±0.3
β	0.686±0.176	0.52±0.12
R^2	0.957	0.921
RSS	77.9	184.9

[a] Parameters are defined in Scheme II. [b]Reactions for the metabolism of testosterone and taxol, respectively, in human liver microsomes, and parameters are defined in Scheme II.

thereby exhibiting substrate-dependent inhibition. This is due to the ESI complex that forms product(s), as measured by factors α and β. The discrepancy in inhibition kinetics between the two substrates is based on the nature of the particular substrate that interacts with the inhibitor in the enzyme. Thus, the size, shape, chemical and physical properties of substrate molecules need to be taken into consideration. In this case, it is obvious that the size difference between testosterone (MW = 288) and taxol (MW = 854) may be one of the key factors to be considered.

Activation

In activation, the activity of a P450 enzyme towards one substrate can be increased in the presence of second substrate [11-14, 26, 29]. Since both molecules are substrates for the enzyme and do not compete with each other, the two-site model may be adapted to interpret activation. Korzekewa *et al.* [12] have developed schemes for several kinetic models and derived a velocity equation for the activation kinetics of α-NF on CYP3A4-catalyzed phenanthrene metabolism, using surface plot fitting. A kinetic model for activation can be projected in many ways in terms

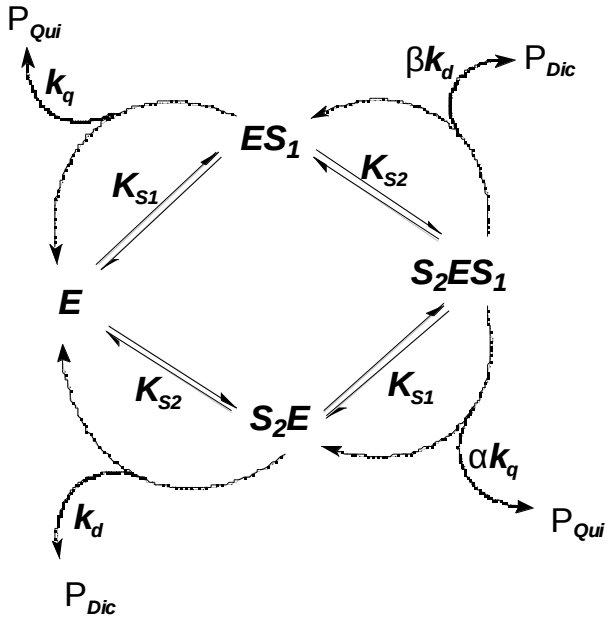

(Scheme VI). Proposed kinetic model for CYP3A4 with two substrate binding domains in the active site applied to the diclofenac-quinidine interaction (activation). Kinetic values are listed in Table 5 (Eqns. 12 and 13).

of the change of apparent K_m and V_{max} observed for each substrate. The CYP3A4-mediated interaction between quinidine and diclofenac is one example of activation [29]. Ngui *et al.* found that (i) quinidine activated the metabolism of diclofenac by increasing significantly the apparent V_{max} (~5-fold) but had no effect on the apparent K_m for diclofenac, and (ii) diclofenac did not alter significantly the apparent K_m but slightly decreased the V_{max} for quinidine. These kinetic interactions can not be explained simply by Michaelis-Menten kinetics using the one binding site model. Thus, a two-site model was proposed, based on changes in apparent kinetic constants, to explain the metabolic fate of the two substrate interaction (Scheme VI). The model postulates that the two different substrate molecules have access to the active site of CYP3A4 and bind simultaneously to the two distinct regions. The two substrates, that bind to their own sites, can be metabolized one at a time. Therefore, substrate and enzyme may be arranged in different combinations (Scheme VI), e.g. ES_1, S_2E and S_1ES_2. Velocity equations for product formation from each substrate are written as Eqn. 12 and 13, from which their kinetic properties, i.e. dissociation (K_S) and rate constants (k_q and k_d) were determined (Table 5).

$$\upsilon_{Qui} = \frac{V_{\max Q}[S_1](K_{S2} + \alpha[S_2])}{K_{S1}K_{S2} + K_{S2}[S_1] + K_{S1}[S_2] + [S_1][S_2]} \quad (12)$$

$$\upsilon_{Dic} = \frac{V_{\max D}[S_2](K_{S1} + \beta[S_1])}{K_{S1}K_{S2} + K_{S2}[S_1] + K_{S1}[S_2] + [S_1][S_2]} \quad (13)$$

where υ_{Qui} and υ_{Dic} are the initial velocities; V_{maxQ} and V_{maxD}, the maximum velocities; k_q and k_d, the rate constants for the formation of 3-hydroxyquinidine and 5-hydroxydiclofenac, respectively; $[S_1]$ and $[S_2]$ are the concentrations of quinidine and diclofenac; K_{S1} and K_{S2}, the dissociation constants for ES_1 and S_2E or S_2ES_1, respectively; α and β are the factors by which V_{max} values are changed for S_2ES_1 when the second molecule is bound. The kinetic constants were determined by the multiple non-linear least-squares algorithm to

Table 5. Calculated Kinetic Parameters for Quinidine-Mediated Activation of Declofenac Metabolism

Substrate	Product	K_{S1} ± S.E.[a] (μM)	K_{S2} ± S.E.[b] (μM)	V_{max} ± S.E.[c] (min^{-1})	Factor[d]	Equation[e]
Quinidine	3-OH-Q (P_{Qui})	1.32±0.19	63.33±9.60	5.92±0.28 (V_{maxQ})	0.61±0.38 (α)	Eqn. 12
Diclofenac	5-OH-D (P_{Dic})	1.42±0.18	54.19±4.78	10.49±1.45 (V_{maxD})	5.87±0.76 (β)	Eqn. 13

[a] K_{S1} = the dissociation constant for $ES_1 \rightleftharpoons E$ and $S_2ES_1 \rightleftharpoons S_2E$ equilibria (see Scheme VI); [b] K_{S2} = the dissociation constant for $S_2E \rightleftharpoons E$ and $S_2ES_1 \rightleftharpoons ES_1$ equilibria; [c] V_{max} = the maximal velocity for the conversion of quinidine to 3-OH-quinidine ($ES_1 \rightarrow P_{Qui}$) or of diclofenac to 5-OH-declofenac ($S_2E \rightarrow P_{Dic}$); [d] Factors by which V_{max} change when the second substrate binds to the enzyme; [e] Equation used for the calculation of kinetic parameters.

describe the kinetic properties for all possible enzyme and substrate complexes. All kinetic parameters in the model were calculated using equation 12 and 13 (Table **5**).

Data fitting to the above model is shown in (Fig. **10A** and **10B**) (R^2 = 0.931 and 0.909, respectively). Two sets of K_{S1} values (1.32 and 1.42 μM) and K_{S2} (63.3 and 54.2 μM), calculated from Eqns. 12 and 13 (Table **5**), were found to be consistent, and represent the binding affinities of quinidine and diclofenac for CYP3A4 either in the presence or absence of the second molecule. In contrast, quinidine exhibited a value for K_S lower than that for diclofenac ($K_{S1} < K_{S2}$). V_{max} values for the formation of 3-OH-quinidine and 5-OH-diclofenac were 5.9 and 10.5 min^{-1}, respectively. Interestingly, the presence of quinidine led to an increase in V_{max} for diclofenac metabolism of 5.9-fold (β = 5.87). However, diclofenac had little effect on the V_{max} for the formation of 3-OH-quinidine (α = 0.61), that resulted in a maximum inhibition by 49%. The results suggest that CYP3A4 contains two distinct binding sites which can be occupied separately by quinidine and diclofenac. The two substrates can not be displaced kinetically by one another as exhibited by the unchanged K_m. However, the site for quinidine appeared to be allosteric, such that the binding of quinidine to the enzyme may change the kinetic characteristics of the second site which preferred diclofenac for metabolism. The kinetic changes at the site could be due largely to the allosteric effect of quinidine at the site that catalyzes diclofenac 5-hydroxylation.

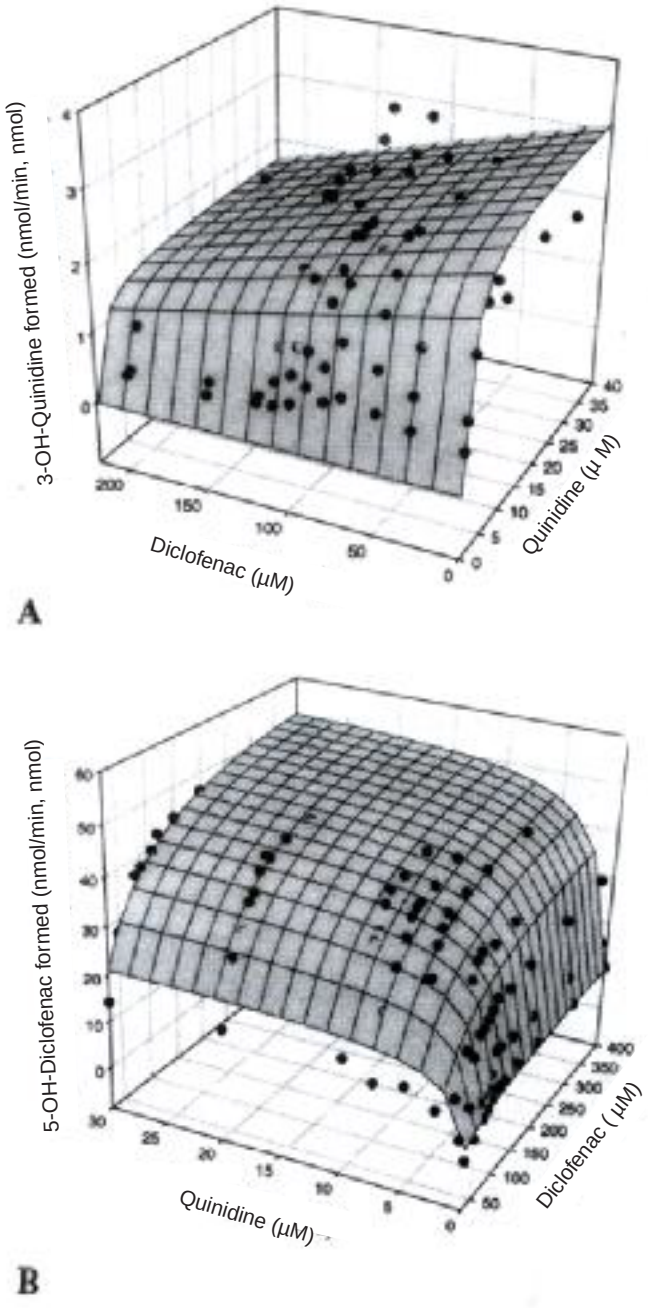

Fig. (10). Activation kinetics for the interaction between quinidine and diclofenac. The surfaces represent the theoretical fits to experimental data (scatter plots). All parameters are given in Table 5 (Eqn. 12 and 13). **A**: Effect of diclofenac on the CYP3A4-mediated formation of 3-hydroxyquinidine and **B**: effect of quinidine on CYP3A4-mediated formation of 5-hydroxydiclofenac.

Differential Kinetics

Differential kinetics occur when an effector (also a substrate) activates the metabolism of a given substrate at one position but inhibits metabolism at a different position. The kinetic scheme is more complicated than any of these discussed above since more product-forming substrate-enzyme complexes can exist. Ueng *et al.* [15] reported that α-NF modulates CYP3A4 catalysis in a regioselective fashion during the oxidation of the carcinogen aflatoxin B_1 [15], resulting in a decrease in the 3α-hydroxylation pathway but an increase in the 8,9-epoxidation reaction. The latter is a metabolic activation pathway of the carcinogenic aflatoxin B1. Similar results have been observed in our study of losartan

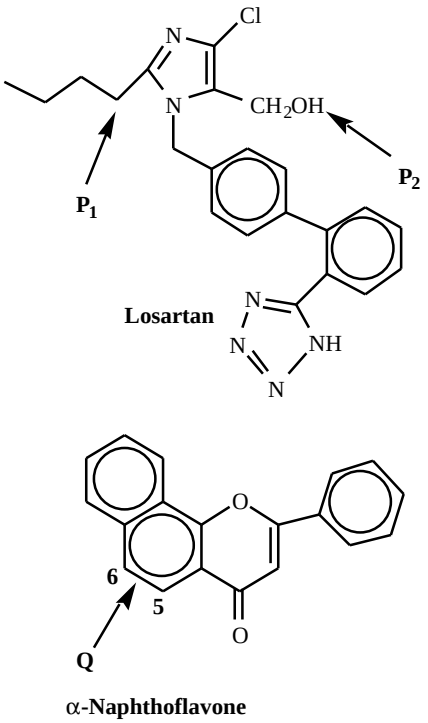

Fig. (11). Structures of losartan and α-NF. Sites of CYP3A4-mediated metabolism are indicated.

metabolism by CYP3A4 [31]. First, α-NF modulates CYP3A4 activity by increasing the formation of the carboxylic acid derivative (P_2, Fig. **11B**) and decreasing the formation of the ω-3 hydroxylated derivative (P_1, Fig. **11A**); second, losartan is an inhibitor of the CYP3A4-mediated formation of the 5,6-epoxide (Q) metabolite of α-NF (Fig. **11** and **12C**); and third, the apparent kinetic constants, e.g. K_m and V_{max}, describing the metabolism of the co-existing substrates are altered significantly by the drug interaction in a manner which could not be described by Michaelis-Menten kinetics. Thus, the two-site model is proposed to address the complexity of this metabolic drug-drug interaction (Scheme VII). The model hypothesizes that CYP3A4 can accommodate two substrate molecules (either the same or different molecular species), simultaneously. The binding orientations of substrate with enzyme are defined on the basis of the metabolic fates of each substrate as presented in Scheme VII. The two occupied binding sites interact kinetically, such that occupancy of the two sites results in changes in the turnover rates of the two substrates, and in the apparent K_m and V_{max} values.

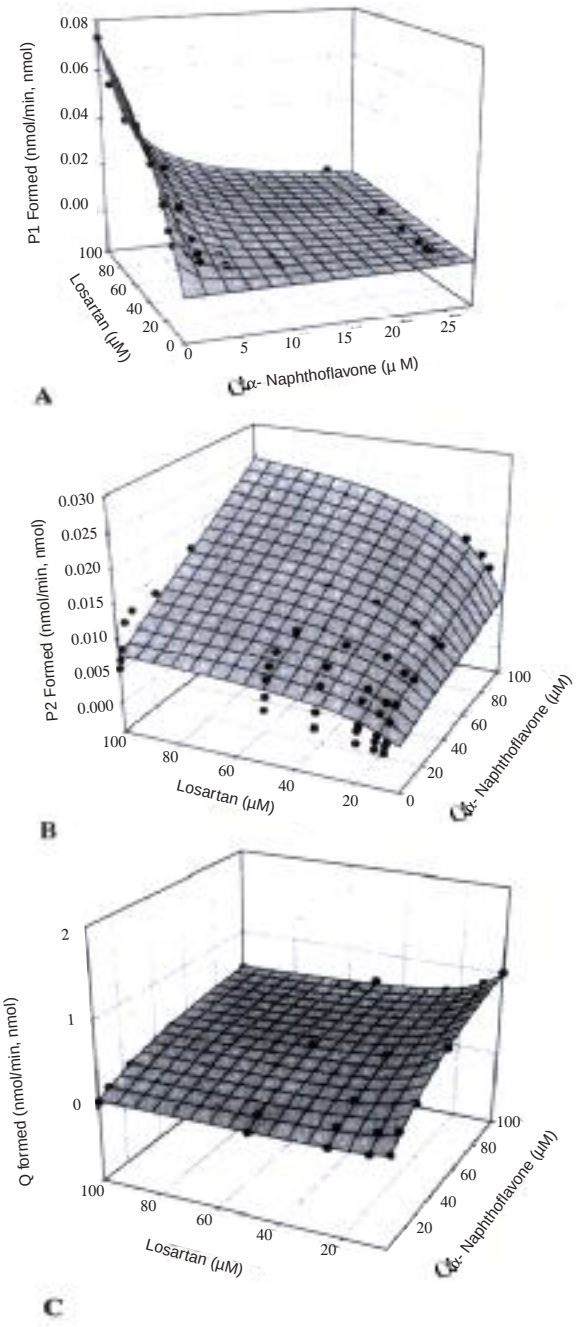

Fig. (12). Kinetics of the CYP3A4-mediated interaction between losartan and α-NF. Data (scatter plots) were predicted from Eqns. 14, 15 and 16, respectively. All calculated kinetic parameters are shown in Table 5. **A**: Effect of α-NF on the CYP3A4-catalyzed formation of ω-3 hydroxy losartan (P_1). The surface plot is a predicted result using Eqn. 14 (RSS = 0.0213, R^2 = 0.992); **B**: effect of α-NF on the CYP3A4-catalyzed formation of the carboxylic acid derivative of losartan (P_2). The surface plot is a predicted result using Eqn. 15 (RSS = 0.101, R^2 = 0.998); and **C**: effect of losartan on the CYP3A4-catalyzed formation of the 5,6-epoxide of α-NF. The surface plot is a predicted result using Eqn. 16 (RSS = 0.0153, R^2 = 0.990).

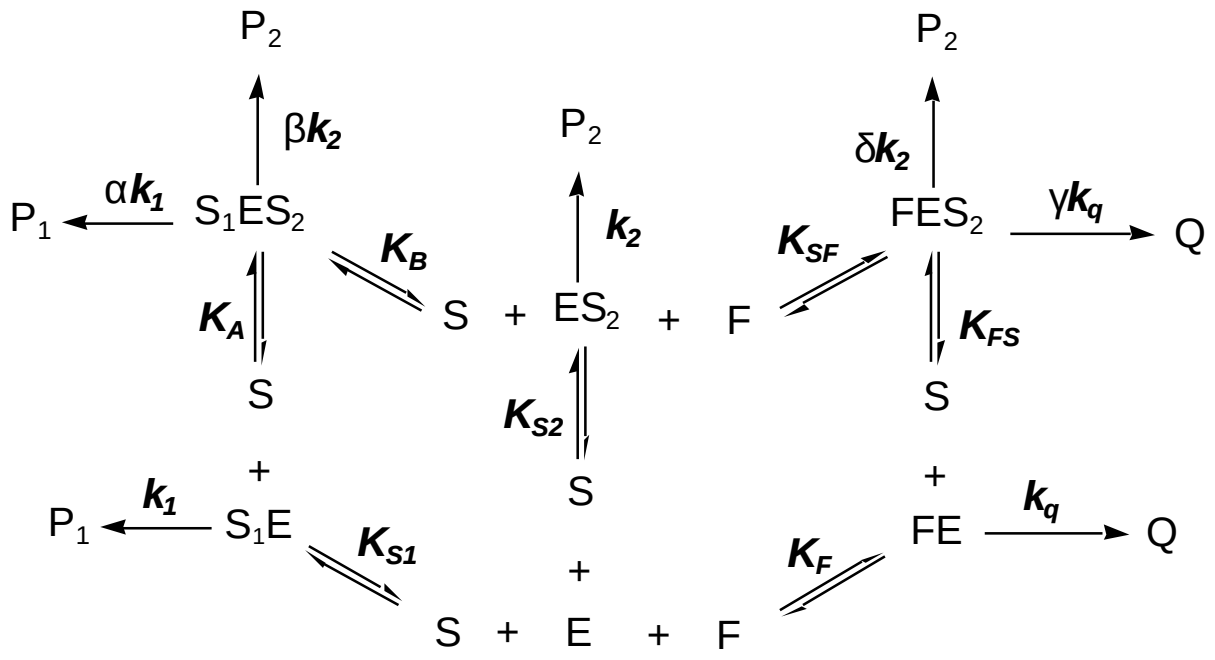

(Scheme VII). Proposed kinetic model for metabolic interaction of simultaneous-existing dual substrates in the active site of CYP3A4 (differetial kinetics). S = losartan; F = α-NF; P_1 = ω-3 hydroxyl losartan; P_2 = losartan carboxylic acid; Q = α-NF-5,6-epoxide; *k* = rate constant; and *K* = dissociation constant. S_1 and S_2 are losartan molecules which bind to the two separate domains, leading to P_1 and P_2 formation, respectivley. Predicted kinetic constants are shown in Table 6 (Eqn. 14, 15 and 16).

Thus, velocity equations for the formation of each major product may be derived (Eqns. 14, 15 and 16), and kinetic estimates that accurately reflect the relationship between substrate(s) and enzyme in any of substrate/effector-enzyme combinations can be obtained (Table **5**).

$$v_{P1} = \frac{V_{\max P1}\left(\frac{1}{K_{S1}} + \frac{\alpha[S]}{K_{S1}K_A}\right)}{\frac{1}{[S]} + \frac{1}{K_{S1}} + \frac{1}{K_{S2}} + \frac{[F]}{K_F[S]} + \frac{[S]}{K_{S1}K_A} + \frac{[F]}{K_{S2}K_{SF}}} \quad (14)$$

$$v_{P2} = \frac{V_{\max P2}\left(\frac{1}{K_{S2}} + \frac{\beta[S]}{K_{S1}K_A} + \frac{\delta[F]}{K_{S2}K_{SF}}\right)}{\frac{1}{[S]} + \frac{1}{K_{S1}} + \frac{1}{K_{S2}} + \frac{[F]}{K_F[S]} + \frac{[S]}{K_{S1}K_A} + \frac{[F]}{K_{S2}K_{SF}}} \quad (15)$$

$$v_Q = \frac{V_{\max Q}\left(\frac{[F]}{K_F[S]} + \frac{\gamma[F]}{K_FK_{FS}}\right)}{\frac{1}{[S]} + \frac{1}{K_{S1}} + \frac{1}{K_{S2}} + \frac{[F]}{K_F[S]} + \frac{[S]}{K_{S2}K_B} + \frac{[F]}{K_FK_{FS}}} \quad (16)$$

In the above equations, [S] and [F] are the concentrations of losartan and α-NF, respectively, and V_{maxP1}, V_{maxP2} and $V_{maxQ,}$ given by $k_1[E]_{total}$, $k_2[E]_{total}$ and $k_q[E]_{total}$, respectively, refer to the maximum velocity of formation of each metabolite at a singly-occupied site. *K* values are dissociation constants for individual enzyme-substrate complexes, while α, β, δ and γ, respectively, represent factors that determine the change in V_{max} at one site when the second site is occupied by the substrate molecule.

(Table **6**) lists all calculated kinetic parameters from the three product velocity equations (Eqns.14-16). α-NF activated the conversion of losartan to P_2 by increasing the V_{max} for FES_2 → FE + P_2 (δV_{maxP2} = 0.032 min^{-1}, δ = 8.3). The resulting value was 8.3-fold greater than V_{maxP2} (0.004 min^{-1}) in the absence of α-NF, implying that the addition of α-NF increases the amount of FES_2 and accelerates the formation of P_2. This suggests that α-NF binding to the one site changes the kinetic properties, exhibited by K_{FS} and factor δ, of the vacant site for losartan which converts losartan preferentially to P_2 in a cooperative manner. However, α-NF inhibited the conversion

Table 6. Predicted Kinetic Parameters for Differential Kinetics of α-NF on the Metabolism of Losartan

Equ.[a]	Prod.[b]	*K* ± S.E.[c]		Factor[d]		*Vmax* ± S.E.[e]		Eqn.
$S_1E \rightleftharpoons E$	P_1	K_{S1}	97±12[f]			V_{maxP1}	0.16±0.04	14
		K_{S1}	67±23					15
		K_{S1}	107±30					16
$S_1ES_2 \rightleftharpoons ES_2$	P_1	K_B	435±108	α	0.38±0.12	αV_{maxP1}	0.06	16, 14
$ES_2 \rightleftharpoons E$	P_2	K_{S2}	25.1±5.6			V_{maxP2}	0.007±0.001	15
		K_{S2}	40.5±1.1					14
		K_{S2}	36.1±3.2					16
$S_1ES_2 \rightleftharpoons S_1E$	P_2	K_A	250±29	β	0.43±0.21	βV_{maxP2}	0.003	15
		K_A	150±45					14
$FES_2 \rightleftharpoons ES_2$	Q	K_{SF}	203±20	γ	0.29±0.11	γV_{maxQ}	1.19	14, 16
		K_{SF}	182±44					15
$FE \rightleftharpoons E$	Q	K_F	183±51			V_{maxQ}	4.1±0.5	16
		K_F	203±89					15
		K_F	158±67					14
$FES_2 \rightleftharpoons FE$	P_2	K_{FS}	15.1±0.8	δ	8.3±2.1	δV_{maxP2}	0.058	16, 15

[a] Enzyme-substrate complexes and their equilibria shown in Scheme VII; [b]Product formed from the specific enzyme-substrate complex. [c]*K* = dissociation constant of each substrate-enzyme complex in the model, calculated by the equations shown above; [d]Factor that determines the change in V_{max} for the first site when the second site is occupied; [e]V_{max} values for that maximum velocity at the specific site of each product-forming complex in the model, calculated by the equations, respectively. *RSS* (residual sum of squares) and R^2 are 0.0213 and 0.992 for Eqn. 14, 0.101 and 0.998 for Eqn. 15, 0.0153 and 0.9899 for Eqn. 16, respectively.

of losartan to P_1, leading to a significant increase in $K_{mP1(app)}$ and a decrease in $V_{maxP1(app)}$ [31]. The differential effect of α-NF suggests that (1) α-NF (F) competes with S_1 at the one site, possibly by a competition between S_1E and FE and between S_1E S_2 and FES_2, leading to a decrease in the formation of product of P_1; and (2) the allosteric effect of α-NF on the other site to which S_2 binds, increases the formation of P_2 ($FES_2 \rightarrow FE + P_2$). Conversely, losartan had similar, but opposite, effects on the kinetic properties of α-NF, such that α-NF metabolism was inhibited by 71% ($\gamma = 0.29$, Table 5) for $FES_2 \rightarrow Q$.

The model also indicates that an interaction occurred when the two substrates (losartan) are identical. As seen in Table 3, K_B for $S_1ES_2 \rightleftharpoons ES_2$ (435 μM) was 4-6.5-fold greater than K_{S1} for $S_1E \rightleftharpoons E$ (67 - 107 μM) but αV_{maxP1} was 38% of V_{maxP1} ($\alpha = 0.38$). Similarly, K_A for $S_1ES_2 \rightleftharpoons S_1E$ (150 - 211 μM) was 3.7 - 8.4-fold higher than K_{S2} for $ES_2 \rightleftharpoons E$ (25 – 40.5 μM), while βV_{maxP2} was 43% of V_{maxP2} ($\beta = 0.43$). These findings illustrate that the two different sites are capable of interacting whenever each is occupied. The appreciable changes in binding affinity and reaction rate for the formation of P_1 and P_2 from losartan are due most likely to the rigidity of the two molecules with a relatively large size (MW = 422) which co-exist at the active site.

CONCLUSIONS

Drug-drug interactions have become an important clinical issue, due to the effects of one drug on the efficacy, toxicity or disposition of another drug. In many cases, drug-drug interactions result in alterations in the pharmacokinetics (metabolic clearance) or pharmacodynamics (antagonistic or additive drug effects) of one or both agents [43-45]. Although interacting agents can affect all aspects of drug disposition, including absorption, distribution, metabolism, and excretion through a variety of mechanisms [47], the most common drug interactions can be understood in terms of alterations in cytochrome P450-catalyzed metabolism. Therefore, the development of kinetic schemes and approximation of constants that can adequately describe the nature of the interaction between the substrates and the enzyme (binding affinity and catalytic capacity) are of considerable value in the prediction of metabolic fate, drug clearance, and the likelihood of clinically important drug-drug interactions. As described herein, application of such models can provide new insights into the mechanism of some unusual drug-drug interactions associated with cytochromes P450, particularly CYP3A4.

ACKNOWLEDGMENT

Authors would like to thank Drs. Kenneth R. Korzekwa and Renke Dai for valuable discussions.

REFERENCES

[1] King, E.L.; and Altaman, C.J. (1956) *J. Phys, Chem*., **60**, 1375-1378.

[2] Hansten, P.D.; and Horn, J.R. (1993) "*Drug interaction and updates*." Applied Therapeutics, Inc., Wancouver, WA.

[3] Nelson, D.R.; Koymans, L.; Kamataki, T.; Stegeman, J.J.; Feyereisen, R.; Waxman, D. J.; Waterman, M. R.; Gotoh, O.; Coon, M.J.; Estabrook, R.W.; Gunsalus, I.C.; and Nebert, D.W. (1996) *Pharmacogenetics*, **6,** 1-42.

[4] Wrighton, S.A.; Stevens, J.C. (1992) The human hepatic cytochromes P450 involved in drug metabolism. *Crit. Rev. Toxicol.*, **22**, 1-21.

[5] Lin, J.H.; Lu, A.Y.H. (1997) *Pharmacol. Rev.*, **49**, 403-449.

[6] Gonzalez, F.J. (1988) *Pharmacol. Rev*., **40**, 243-288.

[7] Guengerich, F.P. (1995) Cytochrome P450: Structure, Mechanism, and Biochemistry. Ed. By Ortiz de Montellano, P.R., pp 473-535, Plenum Press, NY.

[8] Guengerich, F. P. (1988) *Mol. Pharmacol.,* **33,** 500-508.

[9] Guengerich, F.P.; Gillam, E. M. J.; Martin, M.V.; Baba, T.; Kim, B. R.; Raney, K. D.; Yun, C. H. (1994) *Assessment of the Use of Single Cytochrome P450 Enzymes in Drug Research* (Waterman, M.R. and Hildebrand, M. ed), pp. 161-186, Springer, Berlin, Germany.

[10] Segel, I.H. (1975) Enzyme Kinetics: *Behaviour and Analysis of Rapid Equilibrium and Steady State Enzyme Systems*. New York: Wiley & Sons Inc.

[11] Shou, M.; Grogan, J.; Mancewicz, J. A.; Krausz, K. W.; Gonzalez, F. J.; Gelboin, H.V.; Korzekwa, K. R. (1994) *Biochemistry,* **33,** 6450-6455.

[12] Korzekwa, K. R.; Krishnamachary, N.; Shou, M.; Ogai, A.; Parise, R. A.; Rettie, A. E.; Gonzalez, F. J.; Tracy, T. S. (1998) *Biochemistry*, **37**, 4137-4147.

[13] Domanski, T.L.; He, Y-A.; Harlow, G.R.; Halpert, J.R. (2000) *J. Pharmacol. Exp. Ther.,* **293**, 585-591.

[14] Harlow, G.R.; Halpert, J.R. (1998) *Biochemistry,* **95**:6636-6641.

[15] Ueng, Y. G.; Kuwabara, T.; Chun, Y. J.; Guengerich, F. P. (1997) *Biochemistry*, **36,** 370-381.

[16] Shou, M.; Mei, Q.; Ettore, J.R.; M.W.; Dai, R.; Baillie, T. A.; Rushmore, T. H. (1999) *Biochem. J.*, **340,** 845-853.

[17] Schrag, M.L.; Wienkers, L.C. (2000) *Drug Metab. Dispos.*, 29, 70-75.

[18] Lin, Y.; Lu, P.; Tang, C.; Mei, Q.; Rodrigues, A.D.; Rushmore, T.H.; Shou, M. (2001) *Drug Metab. Dispos.*, In press.

[19] Spracklin, D.K.; Hankins, D.C.; Fisher, J.M,; Thummel, K.E.; Kharasch, E.D. (1997) *J. Pharmacol. Exp. Therap.,* **281,** 400-411.

[20] Tang, C.; Shou, M.; Mei, Q.; Rushmore, T.H.; Rodrigues, A.D. (2000) *J. Pharmacol. Exp. Ther.*, **293,** 453-450.

[21] Wang, R.W.; Newton, D.J.; Scheri, T.D.; Lu, A.Y.H. (1997) *Drug Metab. Dispos.*, **25**, 502-507.

[22] Wang, R.W.; Newton, D.J.; Liu, N.; Atkins, W.M.; Lu, Y.H. (2000*) Drug Metab. Dispos.*, **28**, 360-366.

[23] Domanski, T.L.; Lui, J.; Harlow, G.R.; Halpert, J.R. (1998) *Arch. Biochem. Biophys.*, **350**, 223-232.

[24] Ludwig, E.; Schmid, J.; Beschke, K.; Ebner, T. (1999) *J. Pharmacol. Exp. Ther.*, **290,** 1-8.

[25] Maenpaa, J.V.A.A.; Hall, S.D.; Ring, B.J.; Strom, S.C.; Wrighton, S.A. (1998) *Pharmacogenetics,* **8**, 137-155.

[26] Tang, W.; Stearns, R.A.; Kwei, G.Y.; Iliff, S.A.; Miller, R.R.; Egan, M.A.; Yu, N.X.; Dean, D.C.; Kumar, S.; Shou, M.; Lin, J.H.; Baillie, T.A. (1999). *J. Pharmacol. Exp. Ther.*, **291**, 1068-1074.

[27] Schrag, M.L.; Wienkers, L.C. (2000) *Drug Metab. Dispos.*, **28**:1198-1201.

[28] Hosea, N.A.; Miller, G.P.; Guengerich, F.P. (2000) *Biochemistry*, **39,** 5929-5939.

[29] Ngui, J.S.; Tang, W.; Sterrns, R.A.; Shou, M.; Miller, R.R.; Zhang, Y.; Lin, J.H.; Baillie, T.A. (2000) *Drug Metab. Dispos.*, 28, 1043-1050.

[30] Koley, A.P.; Robinson, R.C.; Markowitz, A.; Friedman, F.K. (1997) ; *Biochem. Pharmacol.*, **53**, 455-460.

[31] Shou, M.; Dai, R.; Cui, D.; Korzekwa, K.R.; Baillie, T.A.; Rushmore, T.H. (2001) *J. Biol. Chem.*, 276, 2256-2262.

[32] Lewis, D.F.; Eddershaw, P.J.; Goldfarb, P.S.; Tarbet, M.H. (1996) *Xenobiotica,* **26**, 1067-1086.

[33] Lewis, D.F.V. (1996) Molecular modeling of mammalian cytochromes P450. Cytochromes P450: *Metabolic and Toxicological Aspects* edited by Ioannides, C. CRC Press, Inc. pp 355-398.

[34] Swanson, B.A.; Dutton, D.R.; Lunetta, J.M.; Yang, C.S.; Ortiz de Montellano, P.R. (1991) *J. Biol. Chem.*, **266**, 19258-19310.

[35] Koley, A.P.; Buters, J.T.M.; Robinson, R.C.; Markowitz, A.; Friedman, F.K. (1995) *J. Biol. Chem.*, **270**, 5014-5018.

[36] Koley, A.P.; Robinson, R.C.; Friedman, F.K. (1996) *Biochimie,* **78**, 706-13.

[37] Harlow, G. R.; Halpert, J. R. (1998) *Proc. Natl. Acad. Sci*. USA, **95,** 6636-6641.

[38] Houston, J.B.; Kenworthy, K.E. (2000) *Drug Metab. Dispos.*, **28,** 246-254.

[39] Schwab, G.E.; Raucy, J.L.; Johnson, E.F. (1998) *Mol. Pharmacol.*, **33**, 493-499.

[40] Kerr, B.M.; Thummel, K.E.; Wurden, C.J.; Klein, S.M.; Kroetz, D.L.; Gonzalez, F.J.; Levy, R.H. (1994) *Biochem. Pharmacol.*, **47**,1969-1979.

[41] Schmider, J.; Greenblatt, D.J.; von-Moltke, L.L.; Harmatz, J.S.; Shader, R.I. (1995) *J. Pharmacol. Exp. Ther.*, **275**, 592-597.

[42] Yang, T.J.; Shou, M.; Korzekwa, K.R.; Gonzalez, F.J.; Gelboin, H.V.; Yang, S.K. (1998) *Biochem. Pharmacol.*, **55,** 889-896.

[43] Olkkola, K.T.; Aranko, K.; Luurila, H.; Hiller, A.; Saarnivaara, L.; Himberg, J.J.; Neuvonen, P.J. (1993) *Clin. Pharmacol. Ther.*, **53**, 298-305.

[44] Hardman, J.G.; Limbird, L.E.; Molinoff, P.B.; Ruddon, R.W.; Gilman, A.G. (1996) *The Pharmacological Basis of Therapeutics* (Goodman and Gilman, ed), 9th ed. New York: McGraw Hill.

[45] Honig, P.K.; Wortham, D.C.; Zamani, K.; Conner, D.P.; Mullin, J.C.; Cantilena, L.R. (1993) *J. Am. Med. Assoc.*, **269,** 1513-1518.

[46] Honig, P.K.; Woosley, R.L.; Zamani, K.; Conner, D. P.; Cantilena, L.R. (1992) *Clin. Pharmacol. Ther.*, **52,** 231-238.

[47] Rowland, M.; Tozer, T.N. (1995) Clinical Pharmacokinetics: *Concepts and Applications*. 3rd ed., pp. 267-284, Williams & Wilkins, Baltimore.